Supporting Information

for

Immobilizing Tetraphenylethylene into Fused Metallacycles: Shape Effects on Fluorescence Emission

Zhixuan Zhou,[†] Xuzhou Yan,[*,†,§], Manik Lal Saha,[*,†], Mingming Zhang,[†] Ming Wang,[‡,§] Xiaopeng Li,[‡] and Peter J. Stang[*,†]

[†]*Department of Chemistry, University of Utah, 315 South 1400 East, Room 2020, Salt Lake City, Utah 84112, United States*

[‡]*Department of Chemistry and Biochemistry and Materials Science, Engineering, and Commercialization Program, Texas State University, San Marcos, Texas 78666, United States*

[§]*Current addresses:*

X.Y.: Department of Chemical Engineering, Stanford University, Stanford, California 94305, United States

M.W.: State Key Laboratory of Supramolecular Structure and Materials, College of Chemistry, Jilin University, Changchun, Jilin 130012, R. R. China

Email addresses: xzyan@stanford.edu; manik.saha@utah.edu; stang@chem.utah.edu

1. *Materials and methods*

All reagents were commercially available and used as supplied without further purification. Deuterated solvents were purchased from Cambridge Isotope Laboratory (Andover, MA). Compounds **3**,[1] **4**,[2] and **S1**[3] were prepared according to the published procedures. ^{1}H NMR, ^{13}C NMR and diffusion-ordered (DOSY) NMR spectra were recorded on a Varian Inova 500 MHz spectrometer. ^{31}P{^{1}H} NMR spectra for **5** and **6** were recored on a on a Varian Unity 300 MHz spectrometer. Variable temperature ^{31}P{^{1}H} NMR spectra for **7** and **8** were recorded on a Varian Inova 400 MHz spectrometer. ^{1}H and ^{13}C NMR chemical shifts are reported relative to residual solvent signals, and ^{31}P{^{1}H} NMR chemical shifts are referenced to an external unlocked sample of 85% H_3PO_4 (δ 0.0). Melting points (uncorrected) were obtained with a Mel-Temp capillary melting point apparatus. Mass spectra were recorded on a Micromass Quattro II triple-quadrupole mass spectrometer using electrospray ionization with a MassLynx operating system. Absorption and fluorescence spectra were recorded on a Hitachi U-4100 and Hitachi F-7000 Spectrophotometer, respectively, with aerated spectro-photometric grade solvents at room temperature. The cells used in the experiments were 1 cm quartz cuvettes from Starna Cells, Inc. All samples were freshly prepared for each measurement. The molar absorption coefficients for each solution were calculated using Beer's Law. Quinine sulfate in 0.1 M H_2SO_4 was used to determine the experimental quantum yields at an excitation wavelength of 365 nm with Φ = 0.56 for all assemblies. The quantum yield measurements were performed in multiplicates with values that were within 10 % error being averaged. Dynamic light scattering (DLS) experiments were carried out on a NICOMP 380 particle sizing system at room temperature. All the geometry optimizations were performed at the semi-empirical PM6 level. Furthermore, a refinement of the results was attempted at DFT level, by taking PM6 geometries. Pople's 6-31G** basis set was used for all the main group elements and LANL2DZ basis set was utilized for valance electrons of Pt. To speed up the computation, all the core electrons of Pt were replaced by LANL2DZ effective core potential (ECP). Everything was done by using Gaussian 09 (D.01) program package.

2. *Synthesis and characterization of compounds*

*2.1 Synthesis of ligand **1***

Scheme S1. Synthesis of ligand **1**.

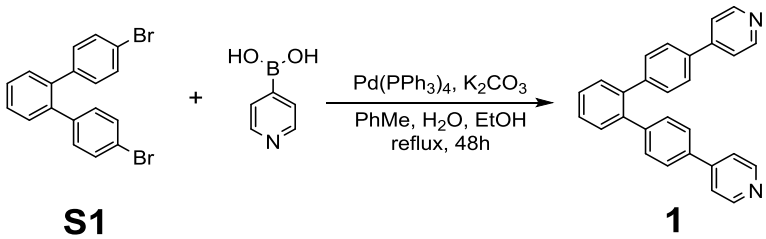

S1 (1.16 g, 2.99 mmol), pyridin-4-yl boronic acid (1.36 g, 11.1 mmol), and $Pd(PPh_3)_4$ (350 mg, 303 μmol) were dissolved in a mixture of toluene (60 mL), EtOH (15 mL) and 2 M potassium carbonate aqueous solution (15 mL). The mixture was stirred at 60 °C for 48 h under nitrogen. After cooling to room temperature, the mixture was poured into water (200 mL) and extracted three times with CH_2Cl_2. The organic layer was dried over anhydrous

sodium sulfate. After removing the solvent under reduced pressure, the residue was chromatographed on a silica gel column with CH_2Cl_2/MeOH (50:1, *v*/*v*) as eluent to give **1** as an off-white solid, Yield: 54%. mp 220-221 °C. The ^{1}H NMR spectrum of **1** is shown in Figure S1. ^{1}H NMR (500 MHz, CD_2Cl_2, 298 K) δ (ppm): 8.62 (d, *J* = 4.9 Hz, 4H), 7.58 (d, *J* = 8.0 Hz, 4H), 7.54-7.44 (m, 8H), 7.33 (d, *J* = 8.0 Hz, 4H). The ^{13}C NMR spectrum of **1** is shown in Figure S2. ^{13}C NMR (125 MHz, CD_2Cl_2, 298 K) δ (ppm): 150.2, 147.4, 142.3, 139.7, 136.1, 130.6, 130.6, 127.9, 126.5, and 121.2. HRMS (ESI-TOF) m/z: $[M+H]^+$ 385.1712.

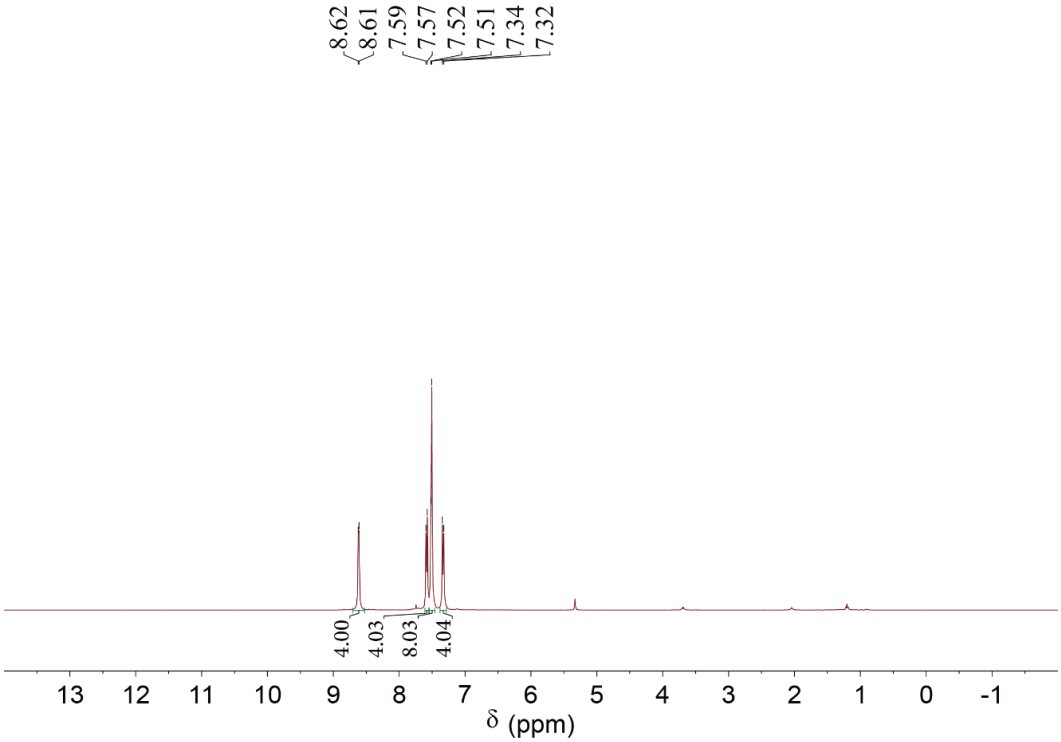

Figure S1. ^{1}H NMR spectrum (500 MHz, CD_2Cl_2, 298 K) of **1**.

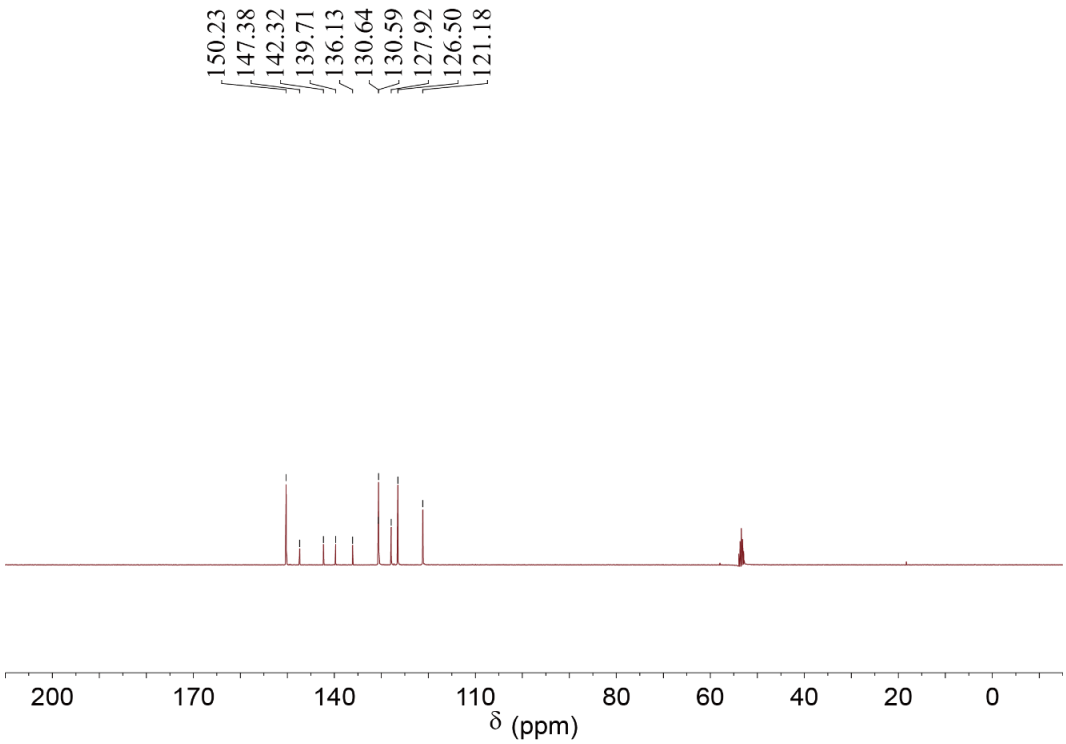

Figure S2. ^{13}C NMR spectrum (125 MHz, CD_2Cl_2, 298 K) of **1**.

*2.2 Synthesis of **5***

Scheme S2. Synthesis of **5**.

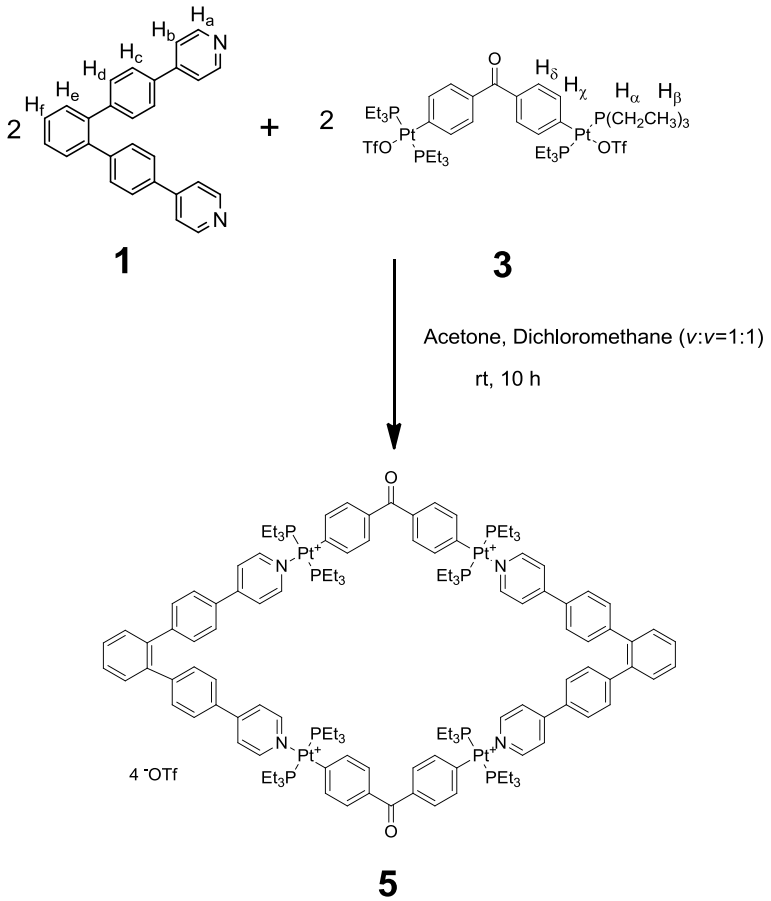

Donor **1** (11.6 mg, 30.2 μmol), acceptor **3** (40.2 mg, 30.0 μmol) were dissolved in 5.0 mL of CH_2Cl_2/CH_3COCH_3 (*v*:*v* = 1:1) in a glass vial. The reaction mixture was allowed to stir for 10 h at room temperature. To the resulting homogeneous solution, diethyl ether was added to precipitate the product, which was then isolated and dried under reduced pressure to give **5** as an off-white solid. **5** was re-dissolved in DMSO-d_6 for characterization. Yield: 95%. The ^1H NMR spectrum of **5** is shown in Figure S3. ^1H NMR (500 MHz, DMSO-d_6, 298 K) δ (ppm): 8.81-8.75 (br, 8H), 8.11-8.04 (br, 8H), 7.98-7.90 (br, 8H), 7.65-7.50 (br, 16H), 7.49-7.28 (br, 16H), 1.38-1.25 (br, 48H), 1.14-0.93 (br, 72H). The $^{31}P\{^1H\}$ NMR spectrum of **5** is shown in Figure S4.$^{31}P\{^1H\}$ NMR (121 MHz, DMSO-d_6, 298 K) δ (ppm): 13.43 (s, $^1J_{Pt\text{-}P}$ = 2634.2 Hz). ESI-TOF-MS is shown in Figure S5: *m*/*z* = 1576.47 $[M–2OTf]^{2+}$, and 1001.32 $[M–3OTf]^{3+}$.

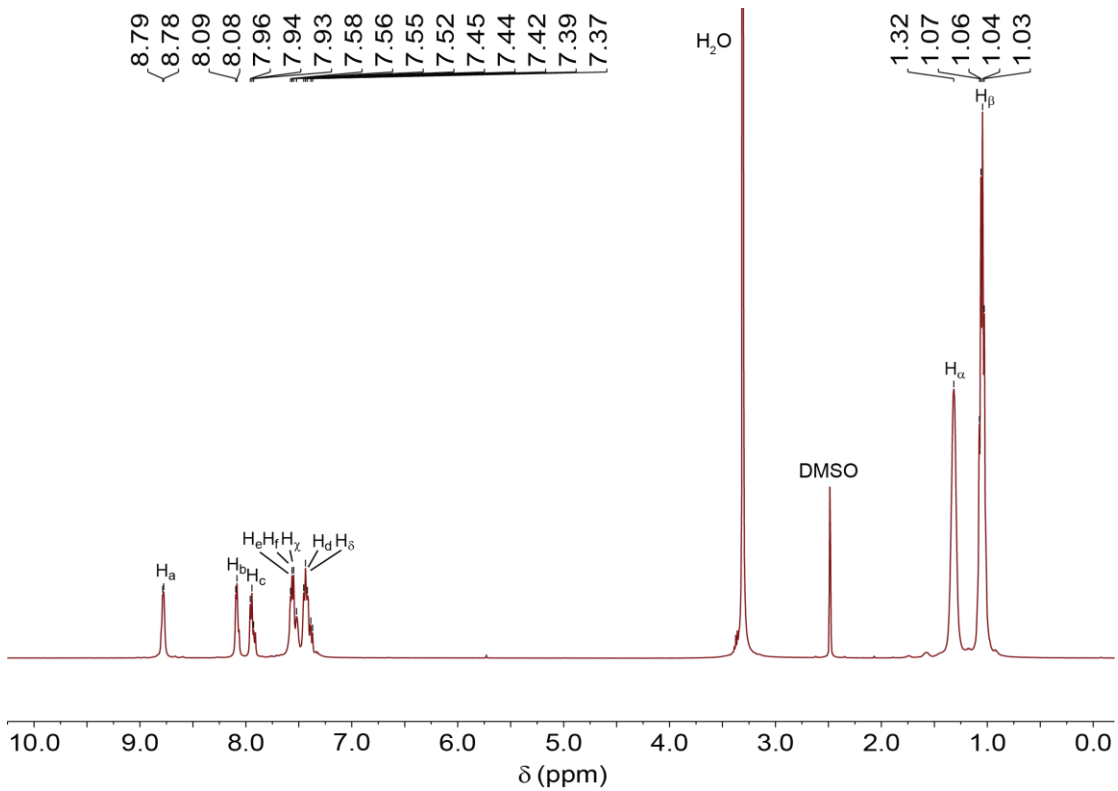

Figure S3. ^{1}H NMR spectrum (500 MHz, DMSO-d_6, 298 K) of rhomboid **5**.

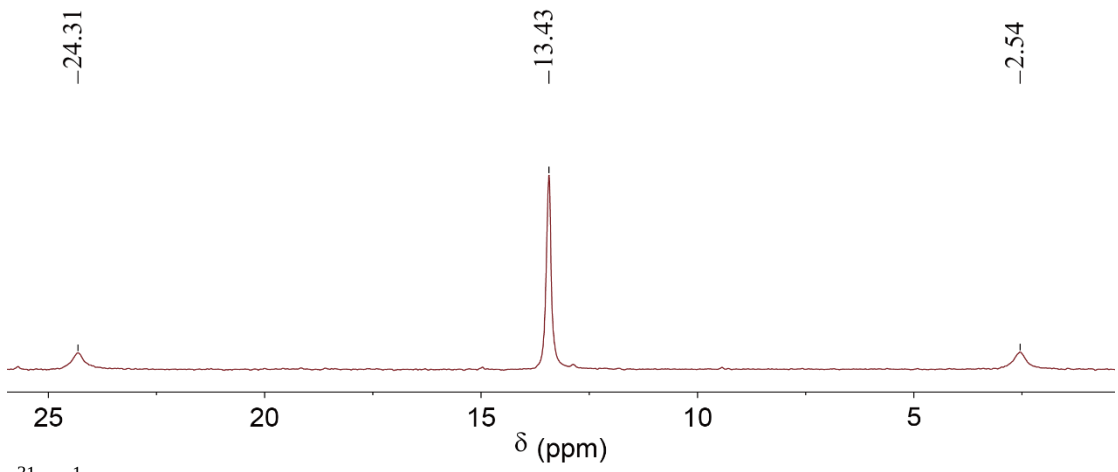

Figure S4. ^{31}P {^{1}H} NMR spectra (121 MHz, DMSO-d_6, 298 K) of rhomboid **5**.

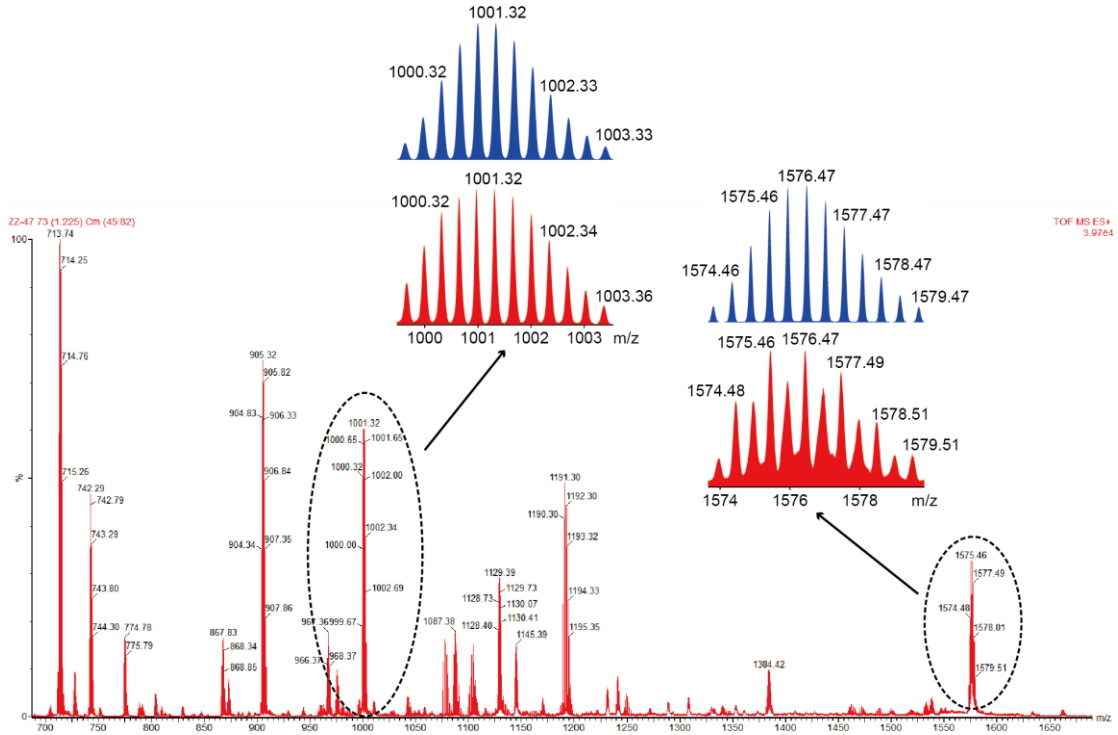

Figure S5. Experimental (red) and calculated (blue) electrospray ionization mass spectrum of rhomboid **5**.

*2.3 Synthesis of **6***

Scheme S3. Synthesis of **6**.

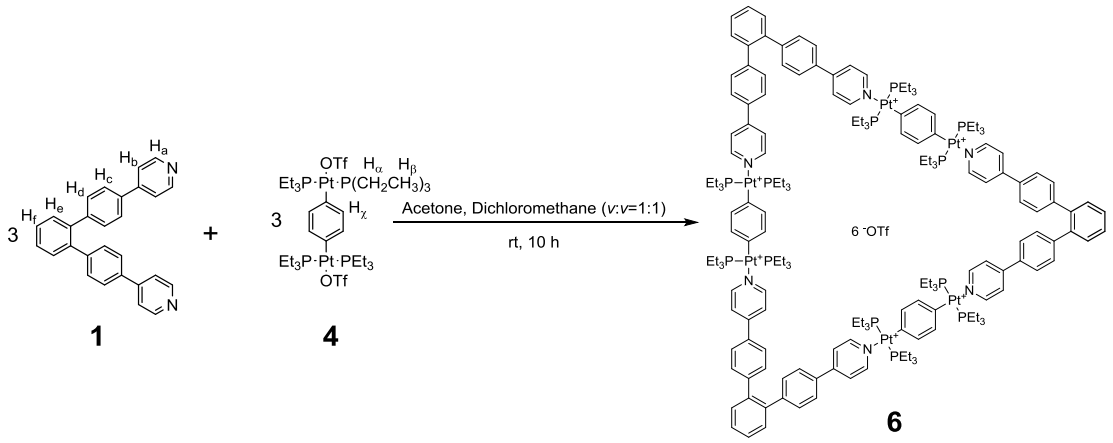

Donor **1** (11.5 mg, 29.9 μmol) and acceptor **4** (37.1 mg, 30.0 μmol) were dissolved in 5.0 mL of CH_2Cl_2/CH_3COCH_3 (*v*:*v* = 1:1) in a glass vial. The reaction mixture was allowed to stir for 10 h at room temperature. To the resulting homogeneous solution, diethyl ether was added to precipitate the product, which was then isolated and dried under reduced pressure to give **6** as an off-white solid. **6** was re-dissolved in DMSO-d_6 for characterization. Yield: 96%. The ^{1}H NMR spectrum of **6** is shown in Figure S6. ^{1}H NMR (500 MHz, DMSO-d_6, 298 K) δ (ppm): 8.73-8.65 (br, 12H), 8.10-8.00 (br, 12H), 7.94-7.85 (br, 12H), 7.59-7.50 (br, 12H), 7.43-7.36 (br, 12H), 6.95 (s, 12H), 1.39-1.20 (br, 72H), 1.15-0.80 (br, 108H). The ^{31}P{^{1}H} NMR spectrum of **6** is shown in Figure S7. ^{31}P{^{1}H} NMR (121 MHz, DMSO-d_6, 298 K) δ (ppm): 13.43 (s, $^1J_{Pt\text{-}P}$ = 2714.0 Hz). ESI-TOF-MS is shown in Figure S8: *m*/*z* = 2282.64 $[M–2OTf]^{2+}$, and 1067.09 $[M–4OTf]^{4+}$.

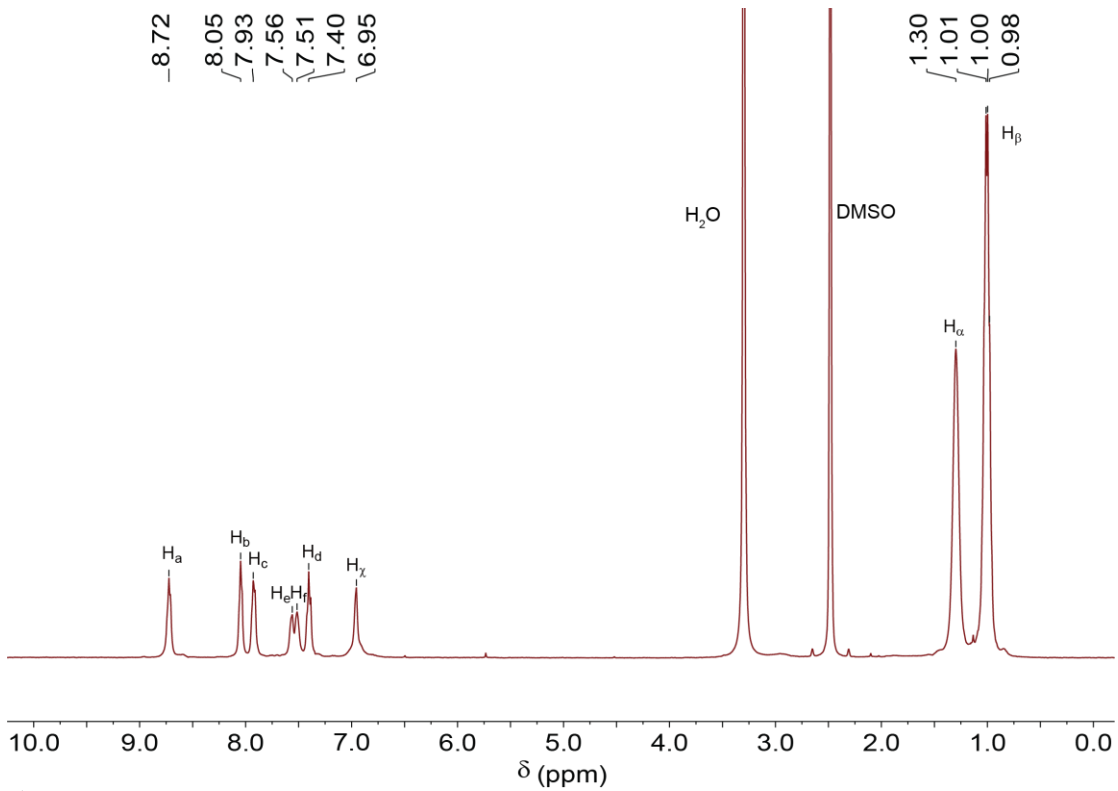

Figure S6. ^{1}H NMR spectrum (500 MHz, DMSO-d_6, 298 K) of triangle **6**.

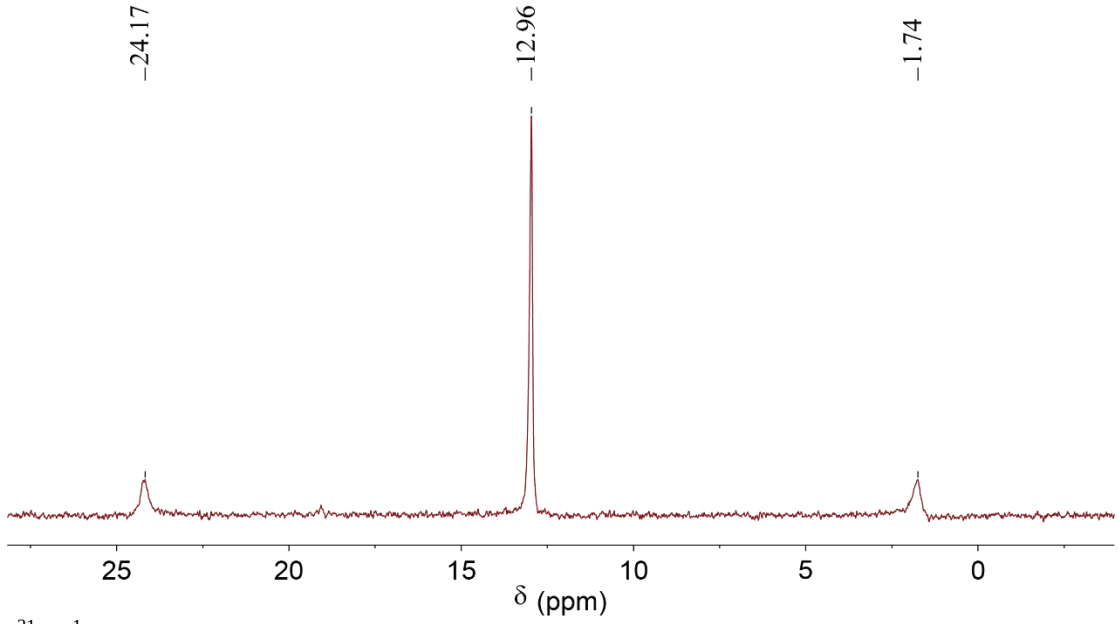

Figure S7. ^{31}P {^{1}H} NMR spectra (121 MHz, DMSO-d_6, 298 K) of triangle **6**.

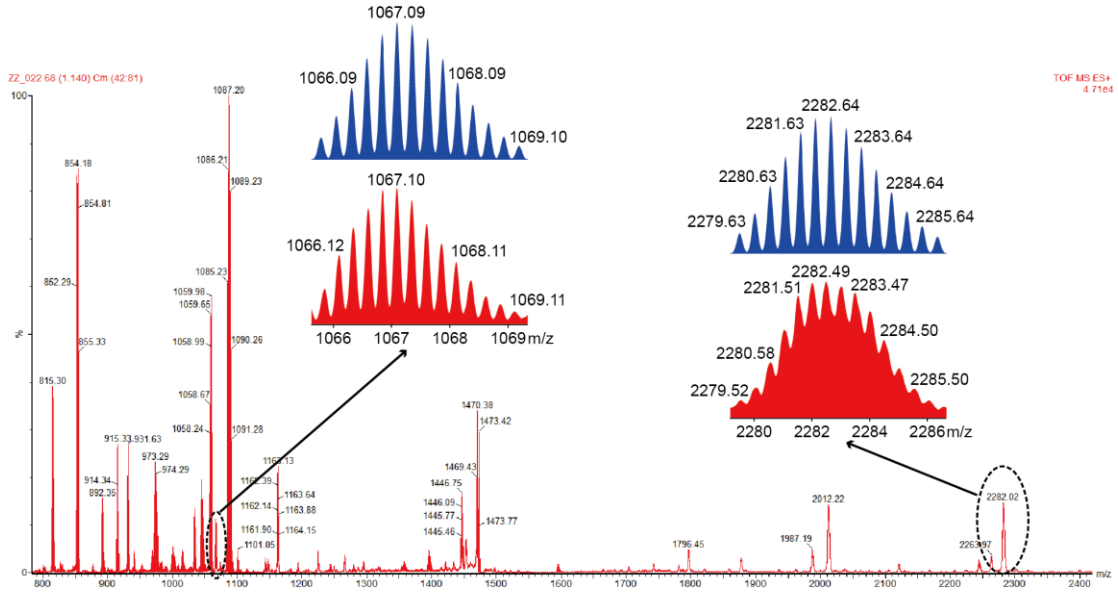

Figure S8. Experimental (red) and calculated (blue) electrospray ionization mass spectrum of triangle **6**.

2.4 Synthesis of 7

Scheme S4. Synthesis of **7**.

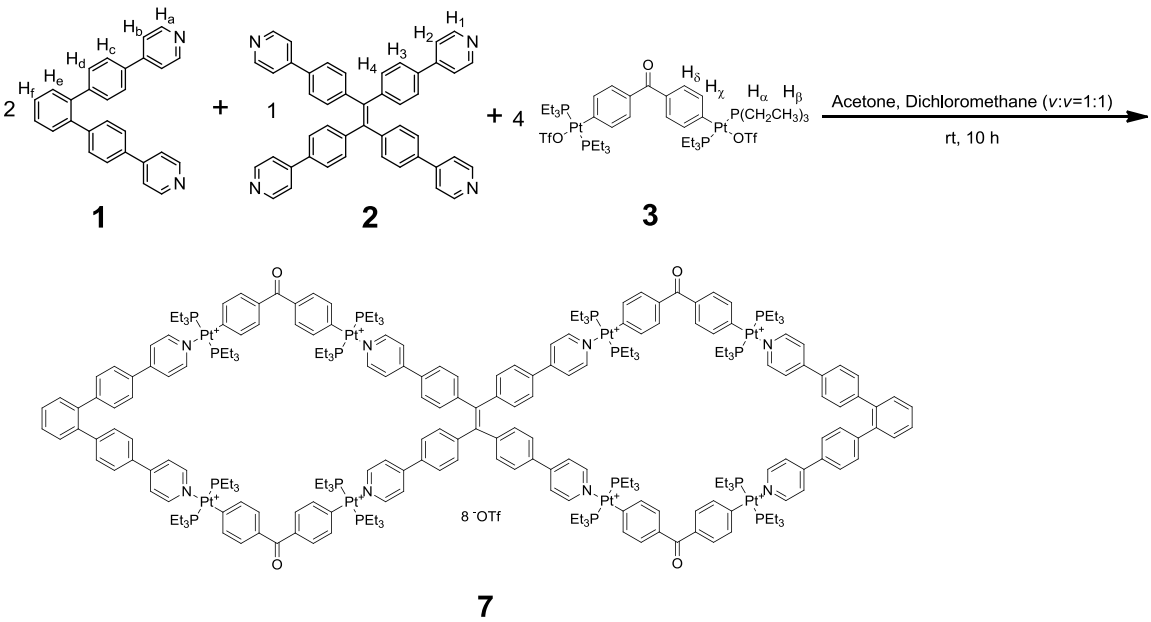

Donor **1** (9.24 mg, 24.0 μmol), donor **2** (7.80 mg, 12.2 μmol) and acceptor **3** (64.4 mg, 48.0 μmol) were dissolved in 5.0 mL of CH_2Cl_2/CH_3COCH_3 (*v*:*v* = 1:1) in a glass vial. The reaction mixture was allowed to stir for 10 h at room temperature. To the resulting homogeneous solution, diethyl ether was added to precipitate the product, which was then isolated and dried under reduced pressure to give **7** as a yellow solid. Yield: 94%. **7** was re-dissolved in DMSO-d_6 for characterization. The ^{1}H NMR spectrum of **7** is shown in Figure S3. ^{1}H NMR (500 MHz, DMSO-d_6, 298 K) δ (ppm): 8.83-8.73 (br, 16H), 8.15-8.00 (br, 16H), 7.98-7.84 (br, 16H), 7.65-7.50 (br, 24H), 7.49-7.28 (br, 32H), 1.39-1.23 (br, 96H), 1.15-0.92 (br, 144H). The ^{31}P{^{1}H} NMR spectrum of **7** is shown in Figure S10.^{31}P{^{1}H} NMR (162 MHz, DMSO-d_6, 323 K) δ (ppm): 13.53, 13.50. ESI-TOF-MS is shown in Figure S11: *m*/*z* = 1205.63 $[M–5OTf]^{5+}$, 979.75 $[M–6OTf]^{6+}$, and 818.66 $[M–7OTf]^{7+}$.

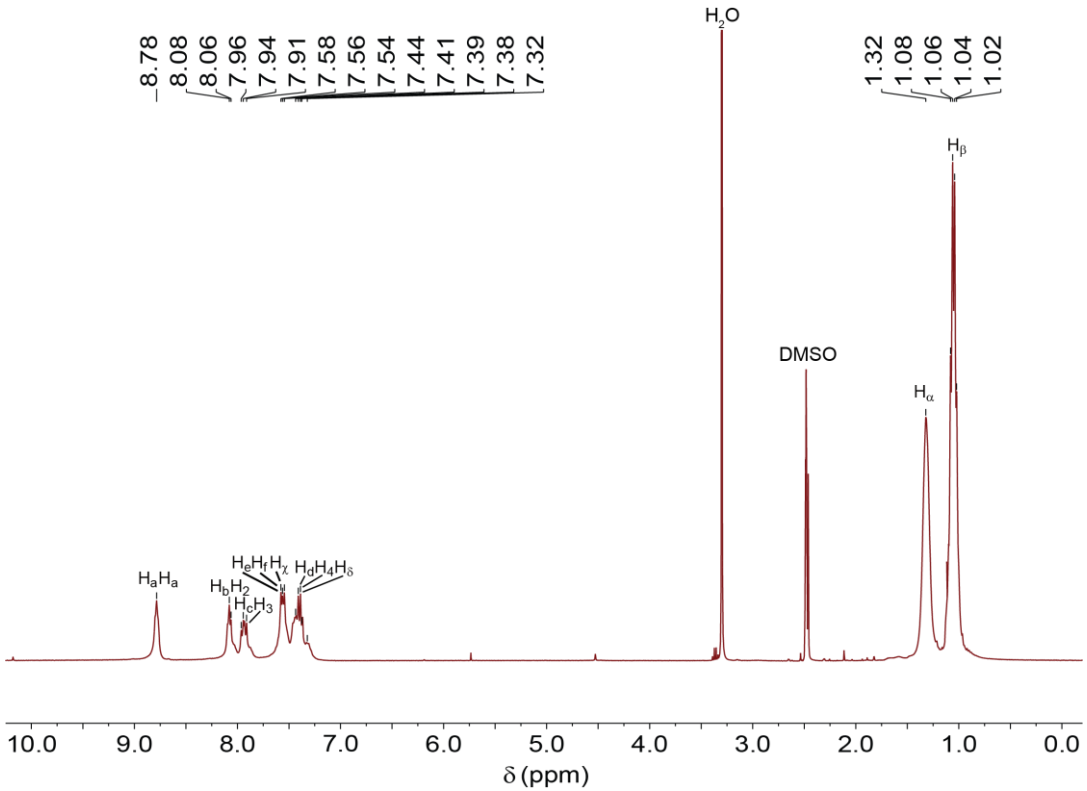

Figure S9. ^{1}H NMR spectrum (500 MHz, DMSO-d_6, 298 K) of **7**.

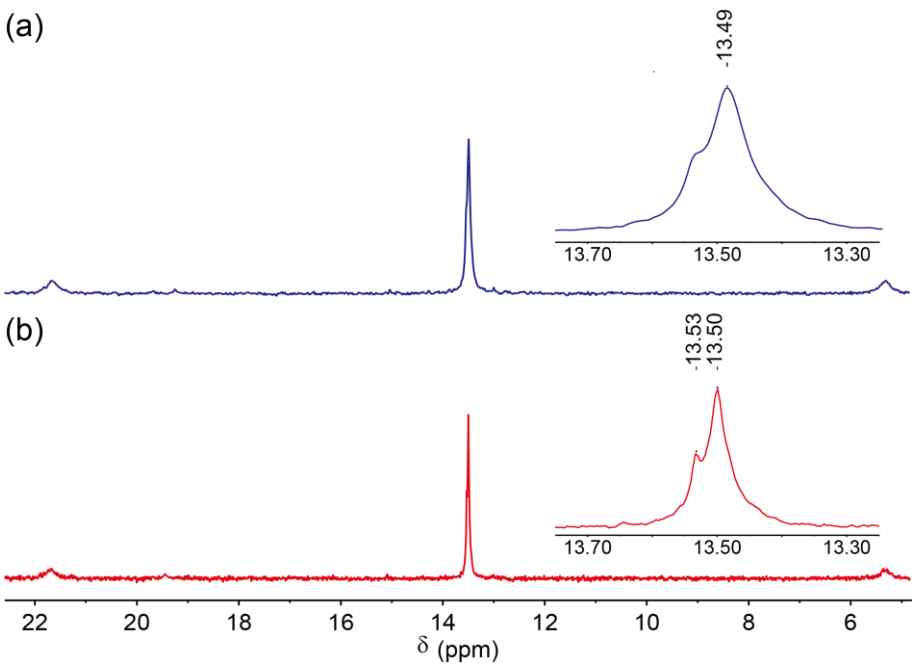

Figure S10. (a) ^{31}P {^{1}H} NMR spectra (162 MHz, DMSO-d_6, 298 K) of double rhomboid **7**. (b) ^{31}P {^{1}H} NMR spectra (162 MHz, DMSO-d_6, 323 K) of double rhomboid **7**.

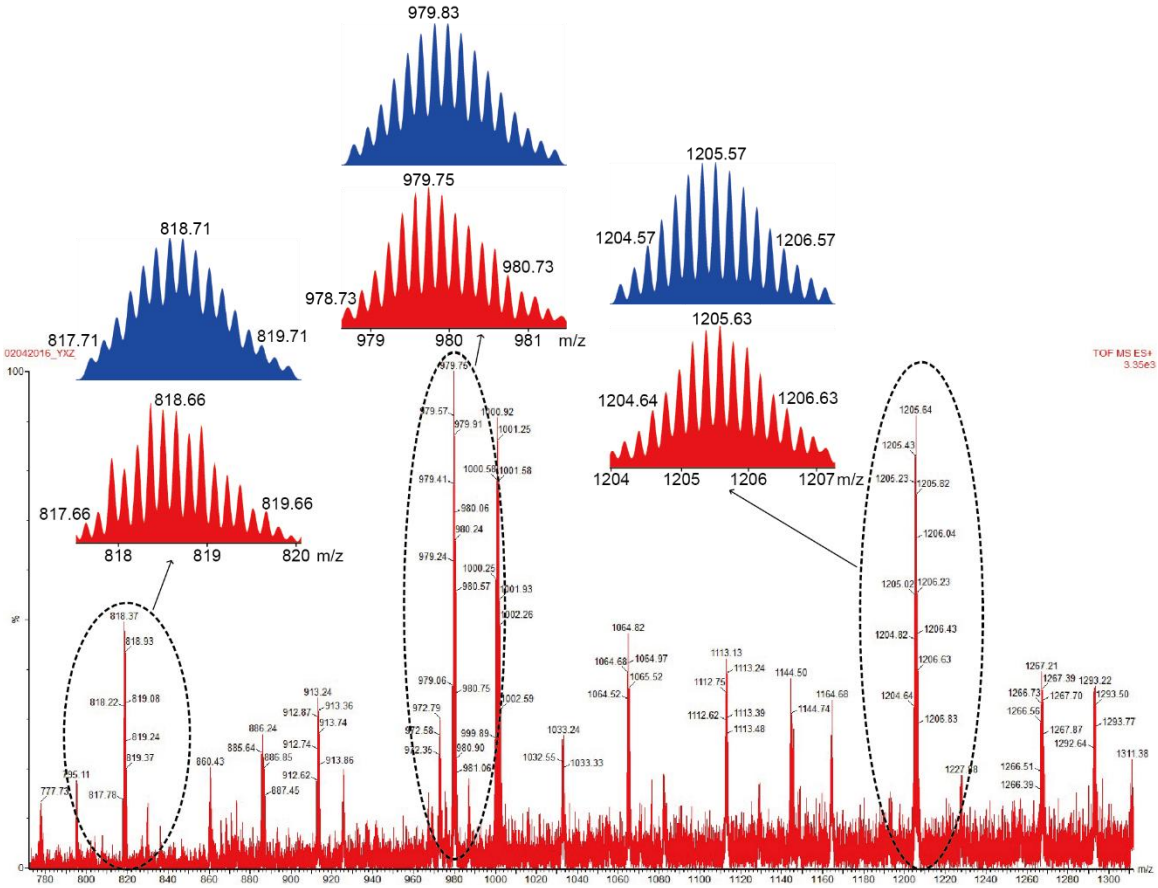

Figure S11. Experimental (red) and calculated (blue) electrospray ionization mass spectrum of **7**.

*2.5 Synthesis of **8***

Scheme S5. Synthesis of **8**.

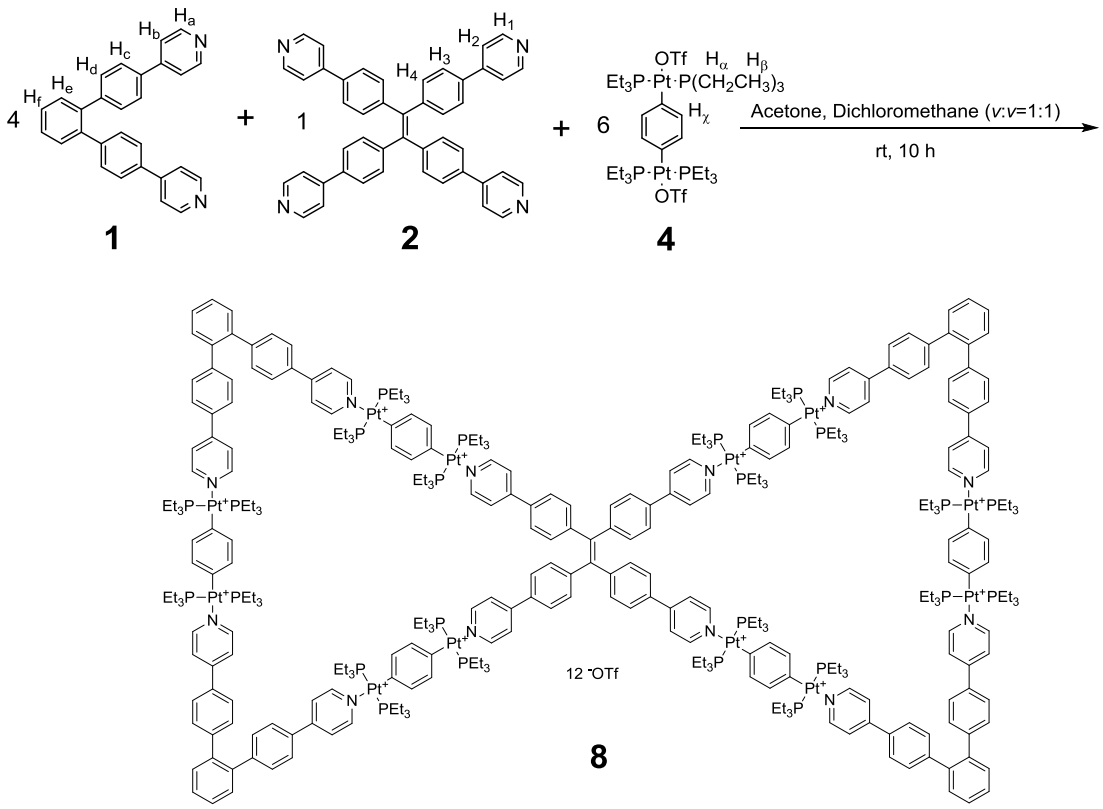

Donor **1** (9.24 mg, 24.0 μmol), donor **2** (3.90 mg, 6.09 μmol) and acceptor **4** (44.5 mg, 36.0 μmol) were dissolved in 5.0 mL of CH_2Cl_2/CH_3COCH_3 (*v*:*v* = 1:1) in a glass vial. The reaction mixture was allowed to stir for 10 h at room temperature. To the resulting homogeneous solution, diethyl ether was added to precipitate the product, which was then isolated and dried under reduced pressure to give **8** as a yellow solid. **8** was re-dissolved in DMSO-d_6 for characterization. Yield: 95%. The ^{1}H NMR spectrum of **8** is shown in Figure S12. ^{1}H NMR (500 MHz, DMSO-d_6, 298 K) δ (ppm): 8.79-8.63 (br, 24H), 8.10-7.98 (br, 24H), 7.95-7.83 (br, 24H), 7.62-7.47 (br, 16H), 7.39 (d, *J* = 7.5 Hz, 16H), 7.34-7.28 (br, 8H), 6.96 (s, 24H), 1.39-1.20 (br, 144H), 1.15-0.80 (br, 216H). The ^{31}P{^{1}H} NMR spectrum of **8** is shown in Figure S13. ^{31}P{^{1}H} NMR (162 MHz, DMSO-d_6, 323 K) δ (ppm): 13.02. ESI-TOF-MS is shown in Figure S14: *m*/*z* = 2249.74 $[M–4OTf]^{4+}$, 1770.47 $[M–5OTf]^{5+}$, and 1450.97 $[M–6OTf]^{6+}$.

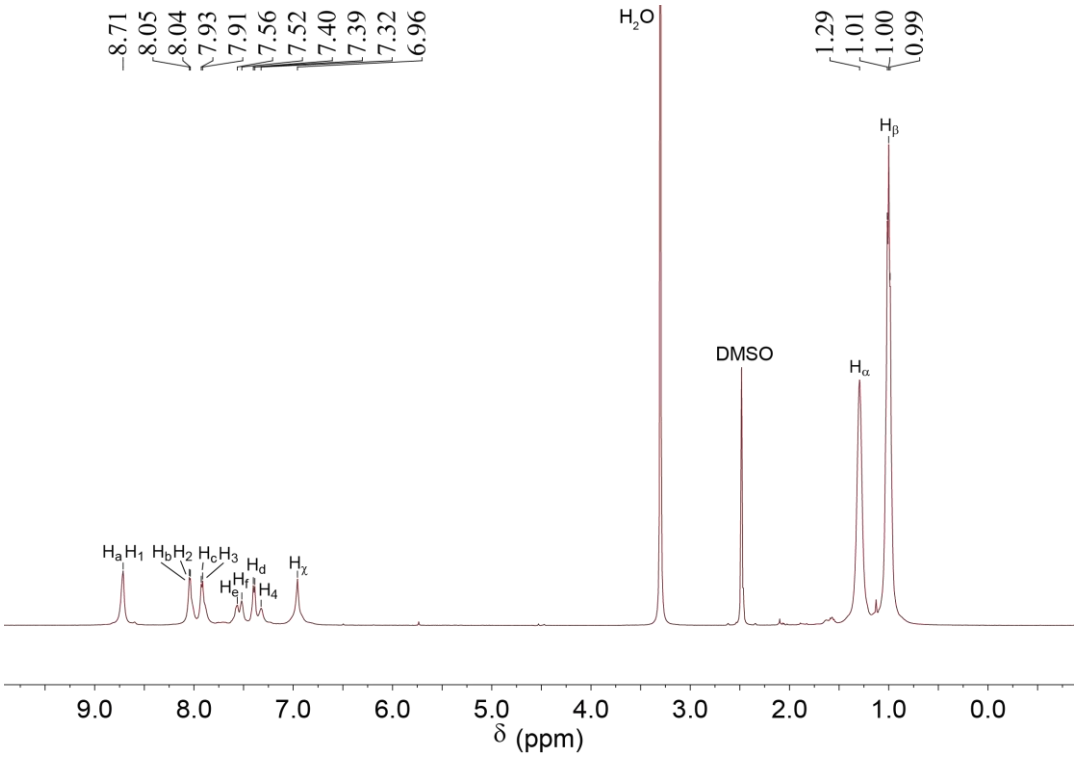

Figure S12. ^{1}H NMR spectrum (500 MHz, DMSO-d_6, 298 K) of **8**.

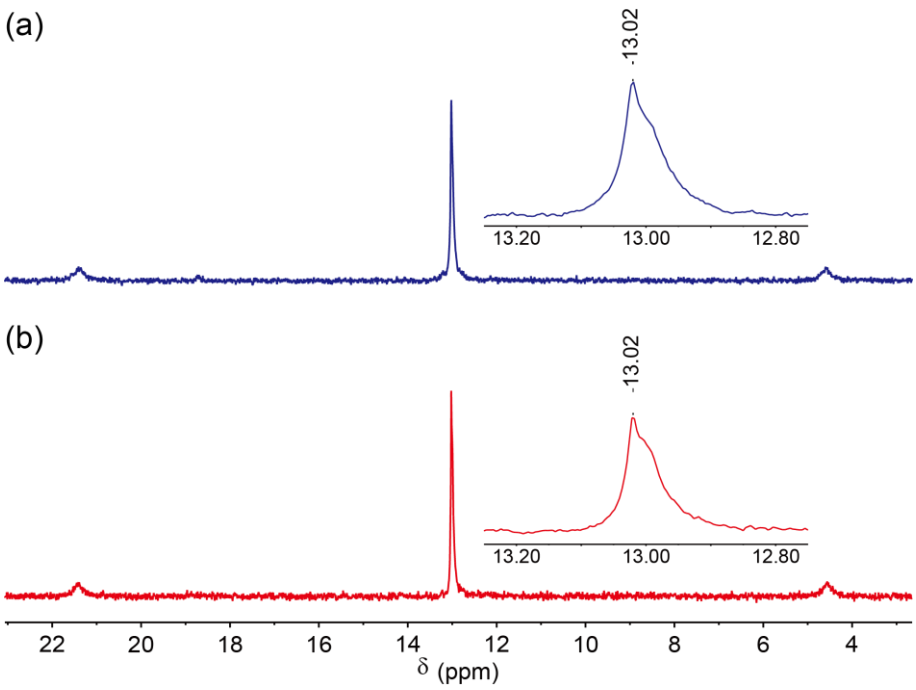

Figure S13. (a) ^{31}P {^{1}H} NMR spectra (162 MHz, DMSO-d_6, 298 K) of double triangle **8**. (b) ^{31}P {^{1}H} NMR spectra (162 MHz, DMSO-d_6, 323 K) of double triangle **8**.

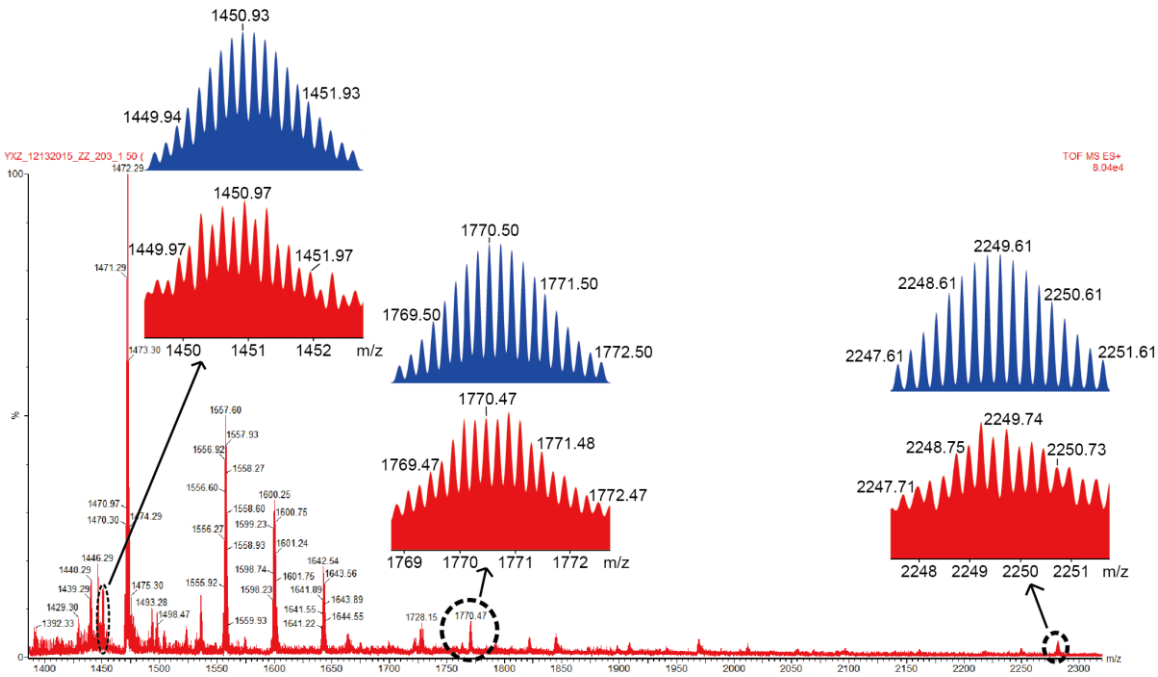

Figure S14. Experimental (red) and calculated (blue) electrospray ionization mass spectrum of **8**.

*3. DOSY NMR experiments of assemblies **5-8**.*

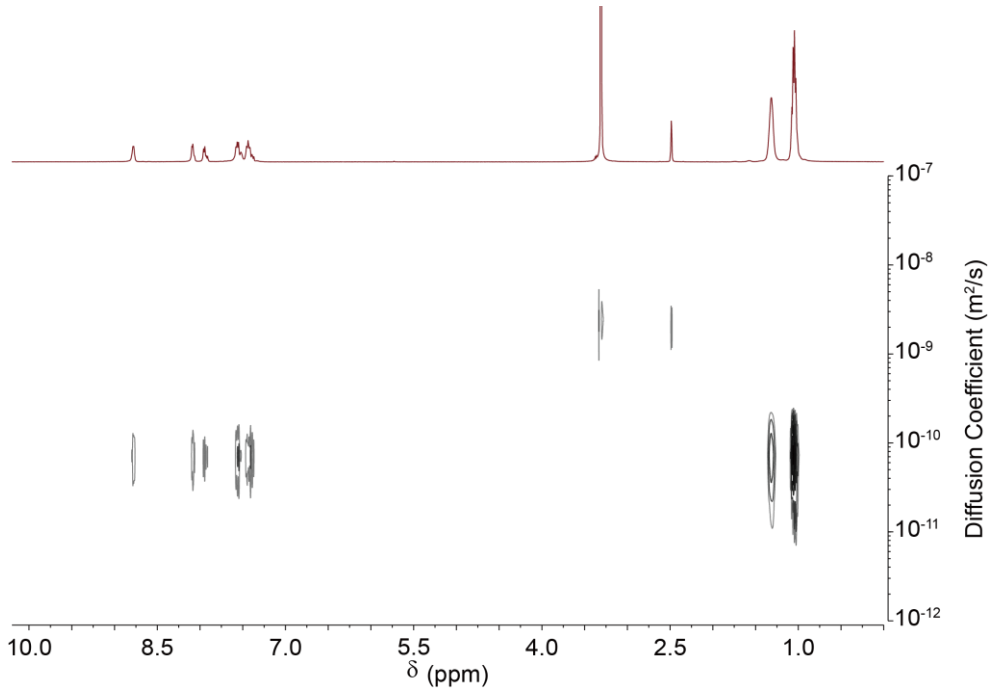

Figure S15. DOSY NMR spectrum (500 MHz, DMSO-d_6, 298 K) of **5**. Diffusion constant D = 6.60×10^{-11} m^2/s. The hydrodynamic radius of the assmbly is 1.66 nm, according to the Stokes-Einstein equation.

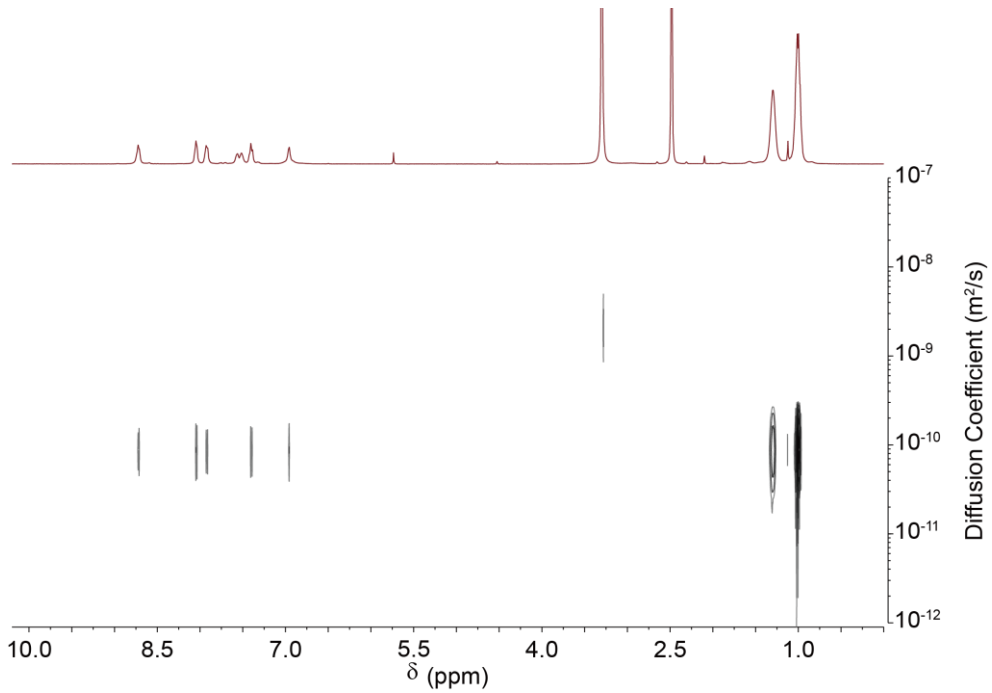

Figure S16. DOSY NMR spectrum (500 MHz, DMSO-d_6, 298 K) of **6**. Diffusion constant D = 8.13×10^{-11} m^2/s. The hydrodynamic radius of the assmbly is 1.35 nm, according to the Stokes-Einstein equation.

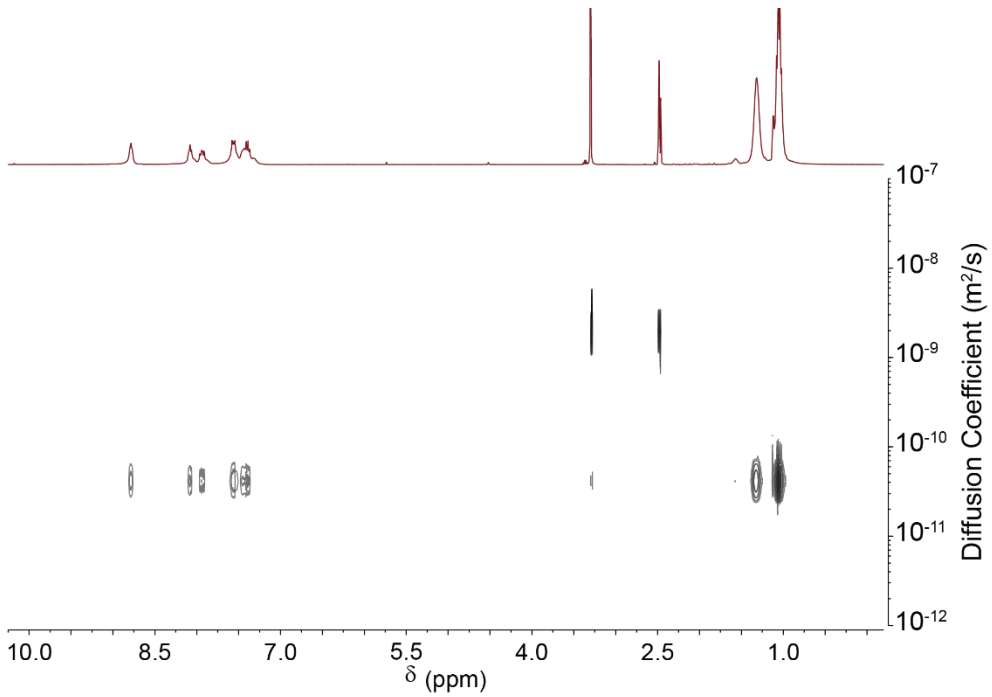

Figure S17. DOSY NMR spectrum (500 MHz, DMSO-d_6, 298 K) of **7**. Diffusion constant D = 4.01×10^{-11} m^2/s. The hydrodynamic radius of the assmbly is 2.73 nm, according to the Stokes-Einstein equation.

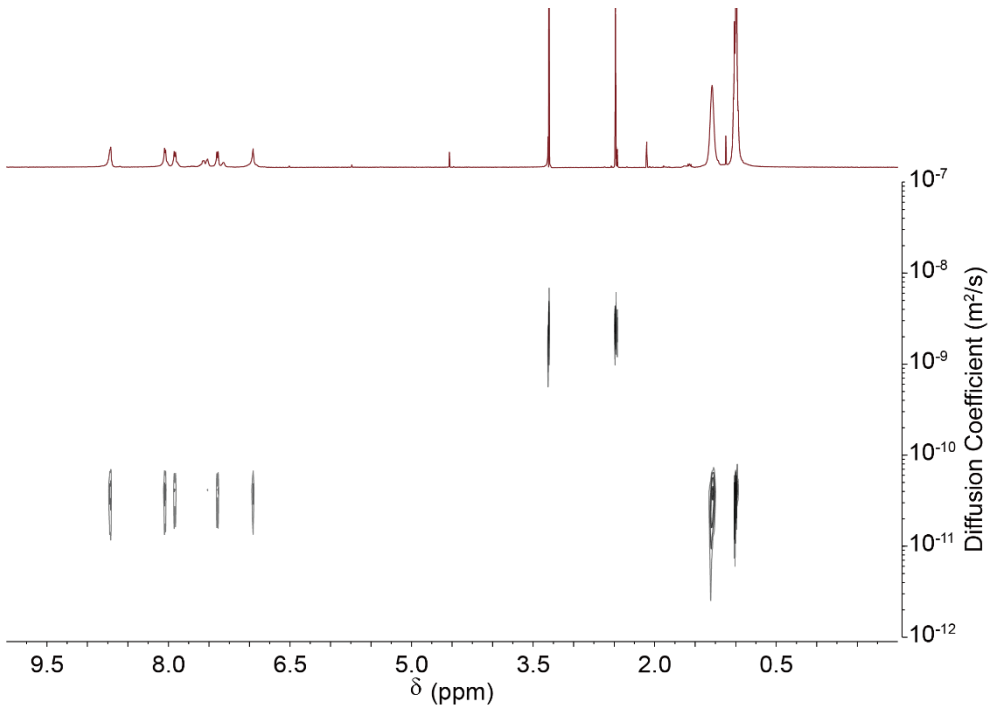

Figure S18. DOSY NMR spectrum (500 MHz, DMSO-d_6, 298 K) of **8**. Diffusion constant D = 3.59×10^{-11} m^2/s. The hydrodynamic radius of the assmbly is 3.05 nm, according to the Stokes-Einstein equation.

*4. Absorption spectra of assemblies **7** and **8** in CH_2Cl_2/hexane mixtures with different hexane contents*

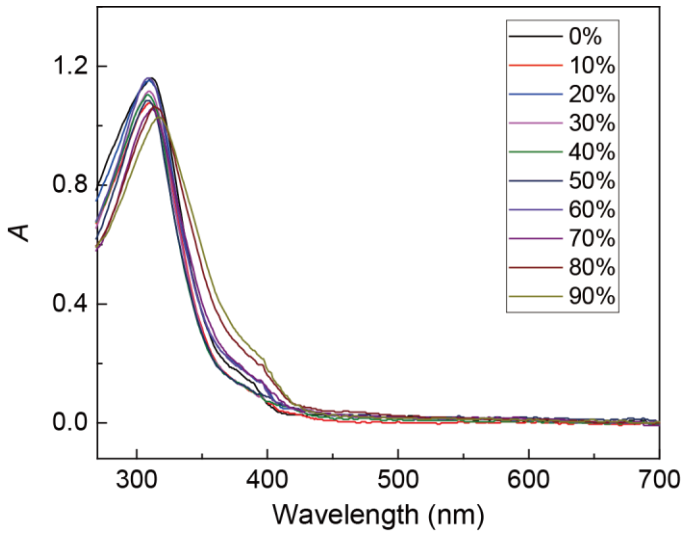

Figure S19. Absorption spectra of **7** in CH_2Cl_2/hexane mixtures with different hexane contents (c = 4.00 μM).

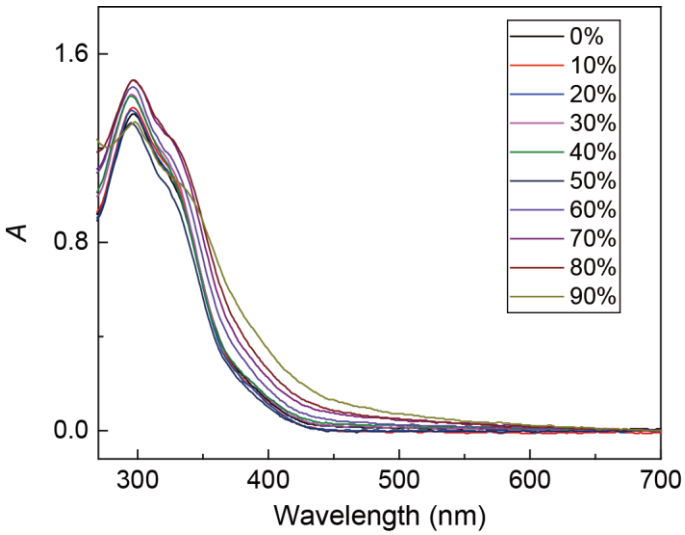

Figure S20. Absorption spectra of **8** in CH_2Cl_2/hexane mixtures with different hexane contents (c = 4.00 μM).

5. *Absorption and emission spectra of **8** in different solvents*

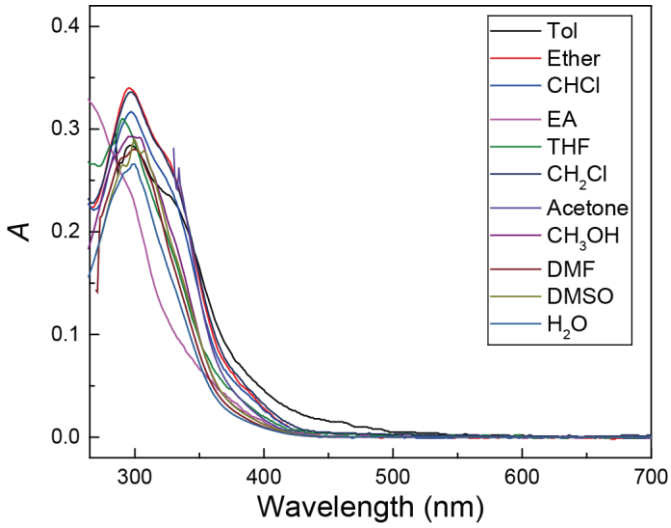

Figure S21. Absorption spectra of **8** in different solvents (c = 1.00 μM). Tol, toluene; EA, ethyl acetate.

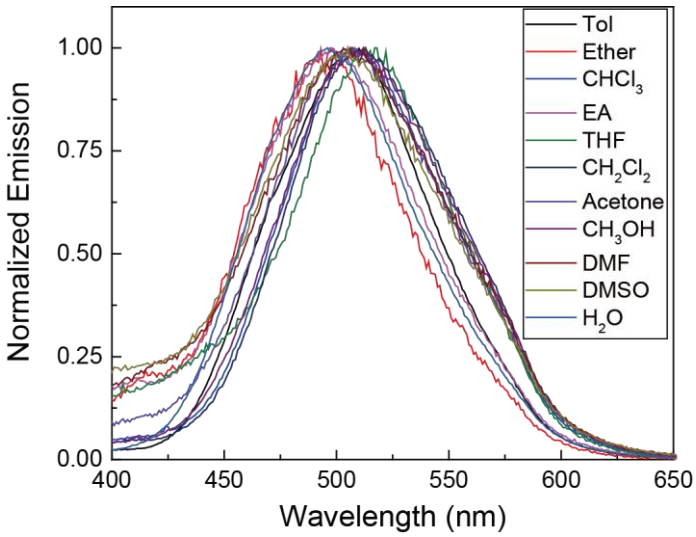

Figure S22. Fluorescence emission spectra of **8** in different solvents (λ_{ex}= 345 nm, c = 1.00 μM). Tol, toluene; EA, ethyl acetate.

Table **S1**. Emission maxima of **8** in different solvents (λ_{ex}= 345 nm, c = 1.00 μM).

Solvent	Toluene	Ether	$CHCl_3$	EA	THF	CH_2Cl_2	Acetone	CH_3OH	DMF	DMSO	H_2O
λ_{max} (nm)	507	498	507	497	512	511	508	512	506	505	498

*6. Absorption and emission spectra of **1** and **3-6***

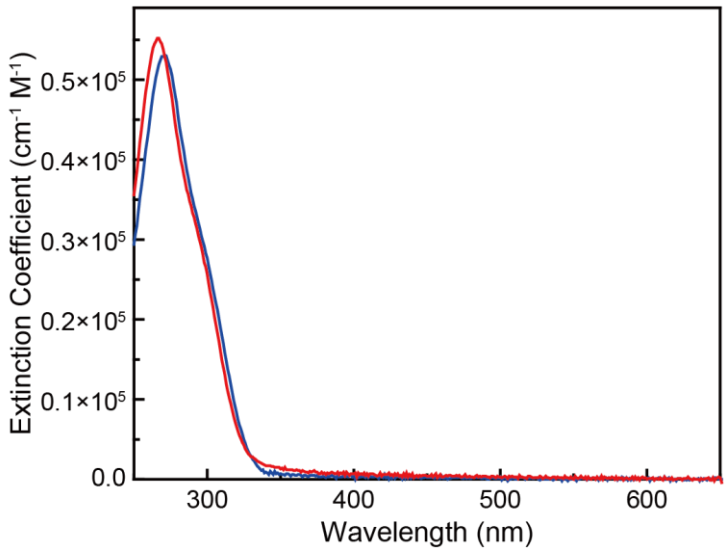

Figure S23. Absorption profiles for **1** in CH_2Cl_2 (blue) and CH_2Cl_2/hexane (10:90 v/v) (red). (c = 4.00 μM).

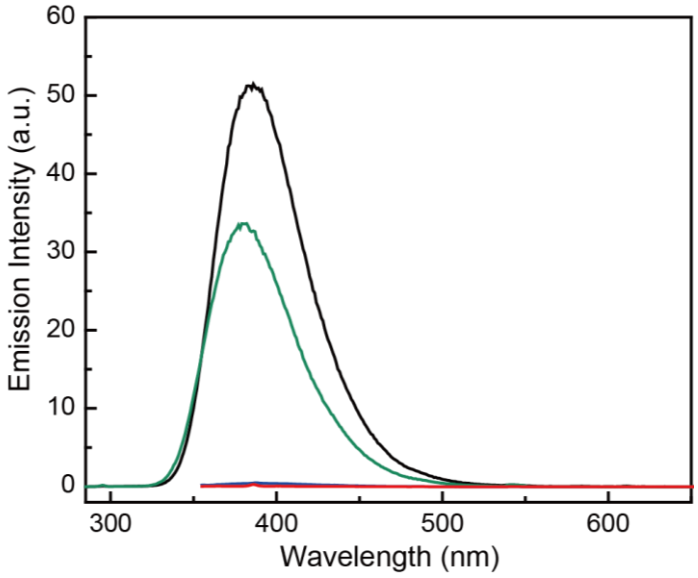

Figure S24. Fluorescence emission spectra: **1** in CH_2Cl_2 (λ_{ex} = 270 nm) (black), **1** in CH_2Cl_2/hexane (10:90 v/v) (λ_{ex} = 270 nm) (green), **1** in CH_2Cl_2 (λ_{ex} = 345 nm) (blue) and **1** in CH_2Cl_2/hexane (10:90 v/v) (λ_{ex} = 345 nm) (red). (c = 4.00 μM).

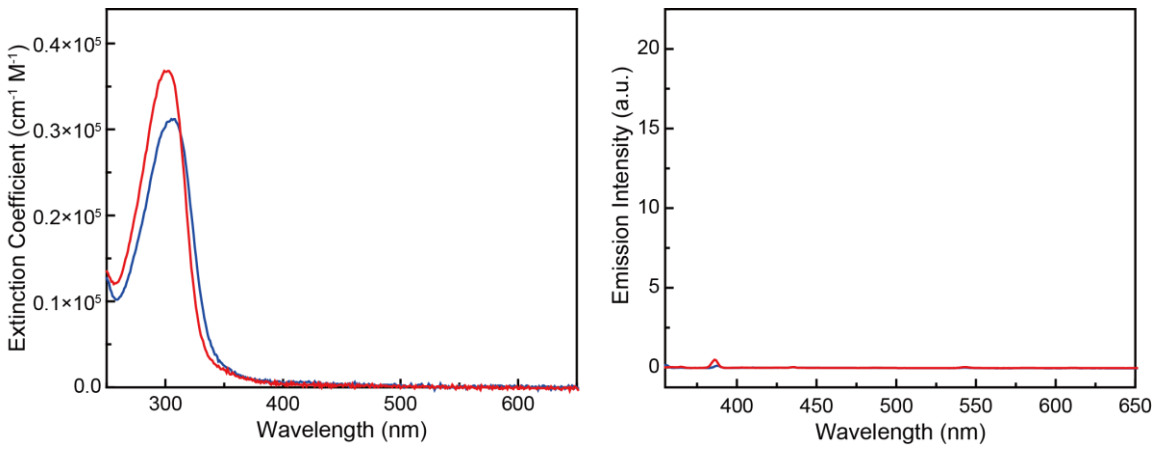

Figure S25. Absorption (left) and emission (right) profiles for **3** in CH_2Cl_2 (blue) and CH_2Cl_2/hexane (10:90 v/v) (red) (λ_{ex} = 345 nm, c = 4.00 μM).

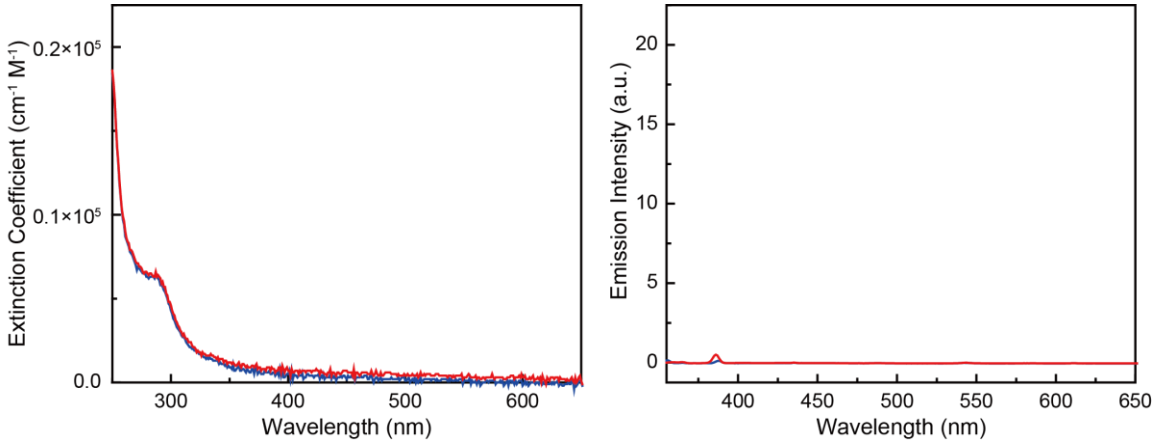

Figure S26. Absorption (left) and emission (right) profiles for **4** in CH_2Cl_2 (blue) and CH_2Cl_2/hexane (10:90 v/v) (red) (λ_{ex} = 345 nm, c = 4.00 μM).

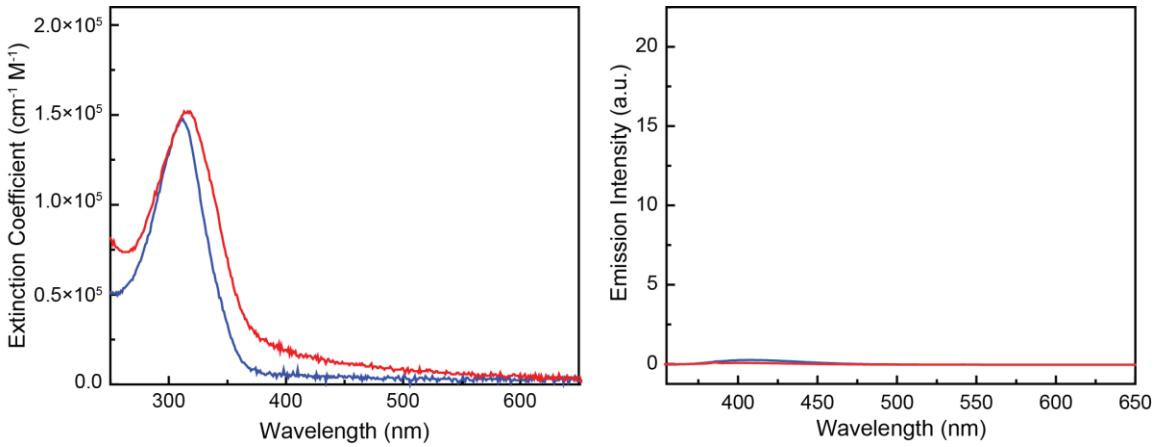

Figure S27. Absorption (left) and emission (right) profiles for **5** in CH_2Cl_2 (blue) and CH_2Cl_2/hexane (10:90 v/v) (red) (λ_{ex} = 345 nm, c = 4.00 μM).

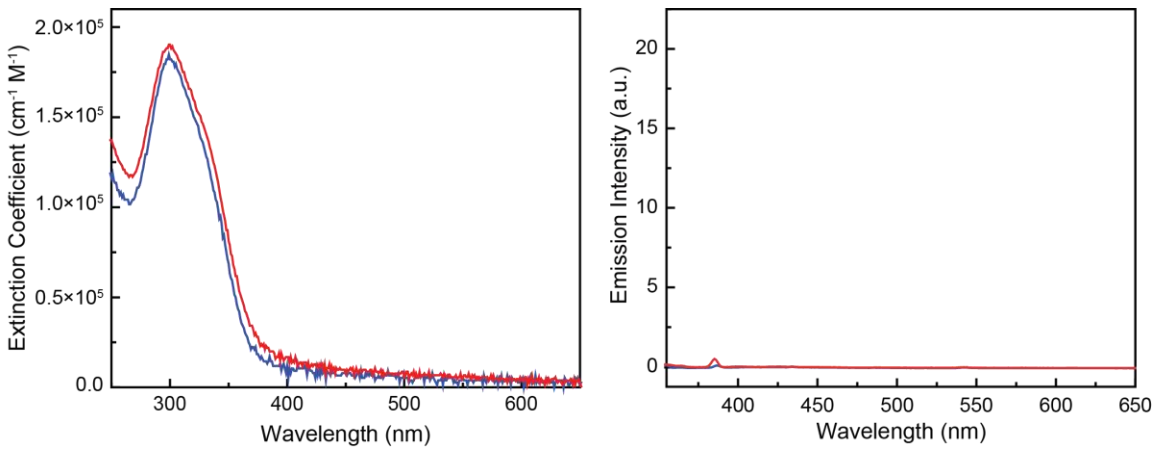

Figure S28. Absorption (left) and emission (right) profiles for **6** in CH_2Cl_2 (blue) and CH_2Cl_2/hexane (10:90 v/v) (red) (λ_{ex} = 345 nm, c = 4.00 μM).

*7. Dynamic light scattering (DLS) data of **7** and **8** in CH_2Cl_2/hexane* (10:90 v/v)

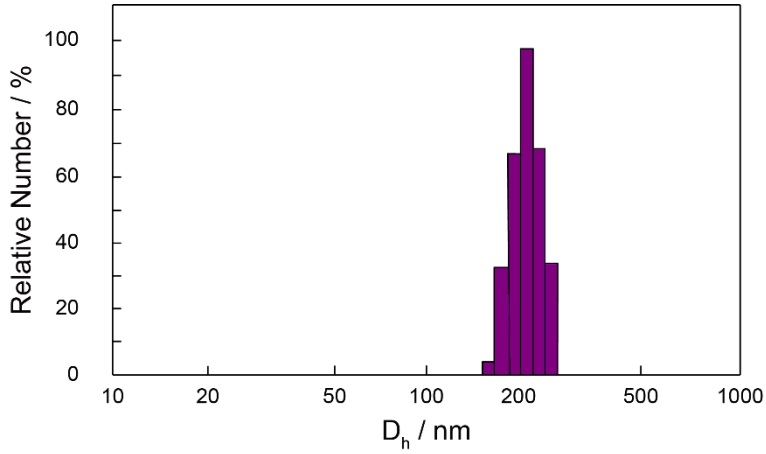

Figure S29. Size distributions of **7** in CH_2Cl_2/hexane (10:90 v/v) at 4.00 μM by DLS. **7** showed a hydrodynamic diameter (D_h) of 210.2 ± 26.3 nm.

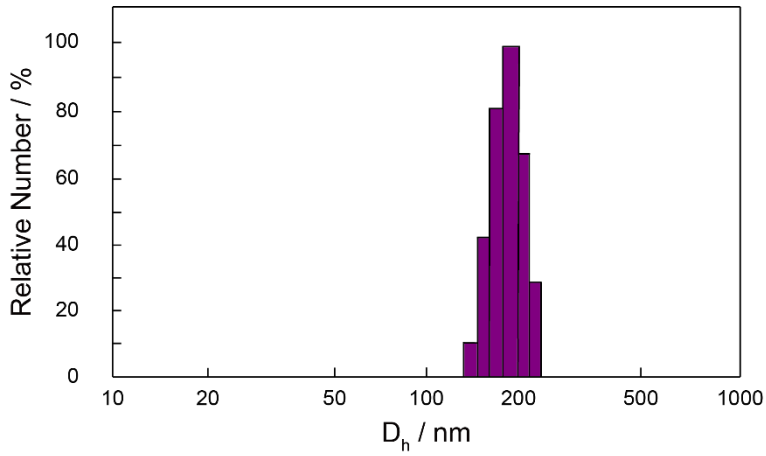

Figure S30. Size distributions of **8** in CH_2Cl_2/hexane (10:90 v/v) at 4.00 μM by DLS. **8** showed a hydrodynamic diameter (D_h) of 180.0 ± 20.0 nm.

8. *DFT/PM6 Computations*

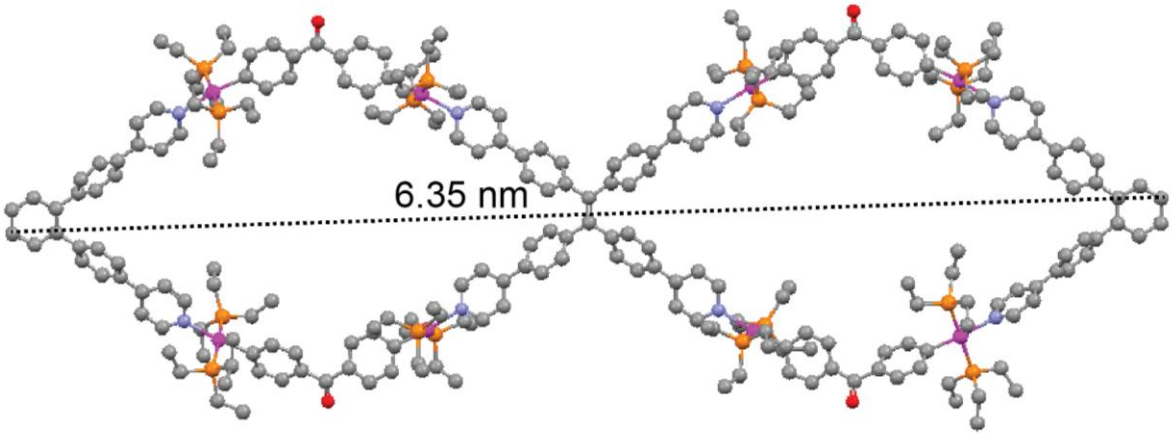

Figure S31. Simulated molecular model of **7** by DFT.

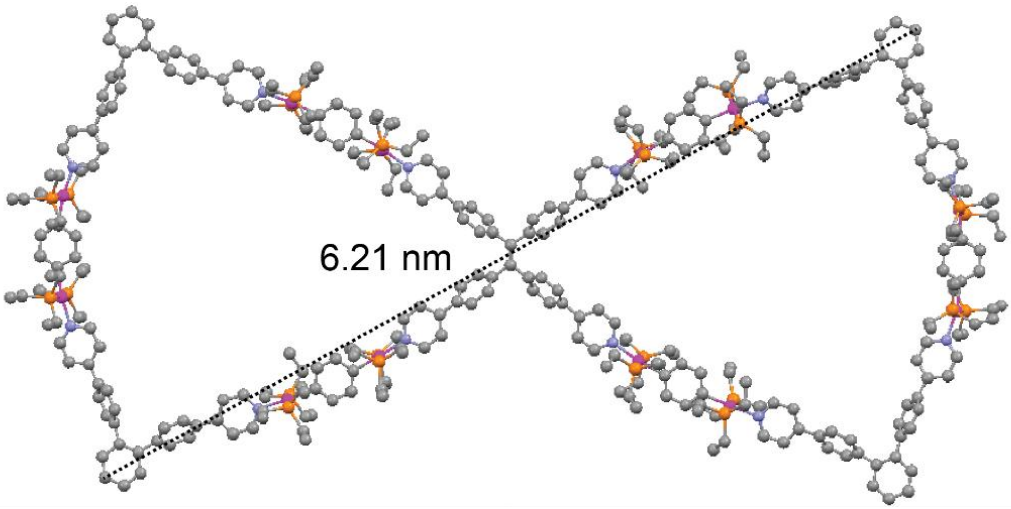

Figure S32. Simulated molecular model of **8** by PM6.

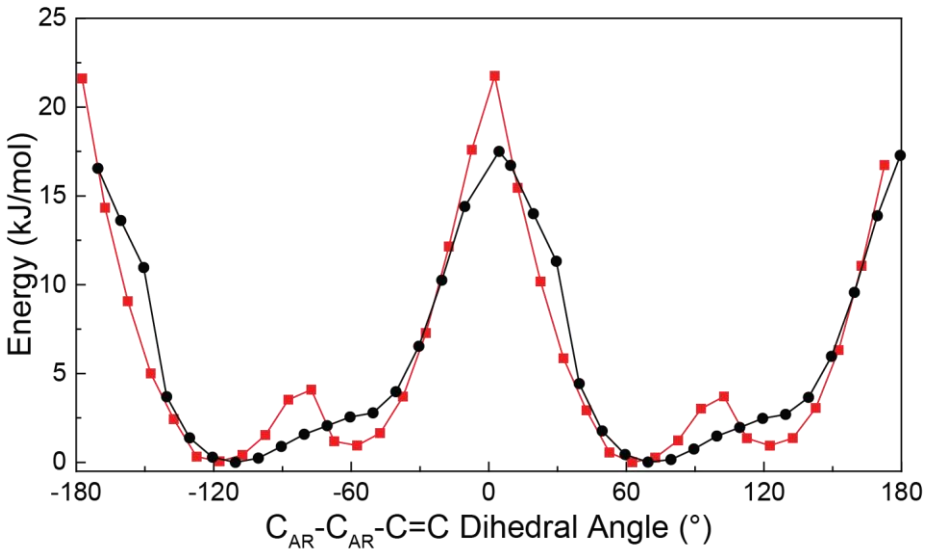

Figure S33. PES for the flipping of one phenyl ring of the TPE moiety within the double rhomboid **7** (black) and the double triangle **8** (red).

References:

1. Yang, H.-B.; Ghosh, K.; Northrop, B. H.; Zheng, Y.-R.; Lyndon, M. M.; Muddiman, D. C.; Stang, P. J. *J. Am. Chem. Soc.* **2007**, *129*, 14187.

2. Manna, J.; Kuehl, C. J.; Whiteford, J. A.; Stang, P. J.; Muddima, D. C.; Hofstadler, S. A.; Smith, R. D. *J. Am. Chem. Soc.* **1997**, *119*, 11611.

3. Sakamoto, Y.; Suzuki, T. *J. Am. Chem. Soc.* **2013**, *135*, 14074.